*Egypt. J. Chem.* **Vol. 64**, No. 1 pp. 93 - 105 (2021)

# Egyptian Journal of Chemistry

**http://ejchem.journals.ekb.eg/**

## 3D-Molecular Modeling, Antibacterial Activity and Molecular Docking Studies of Some Imidazole Derivatives

**Dhafer S. Zinad[a,*], Ahmed Mahal[b,c,d,*], Abdulqader M. A-Qader[e], Siswandono Siswodihardjo[f], Mohammad Rizki Fadhil Pratama[g,h], Ranjan K. Mohapatra[i]**

[a] Applied Science Department, University of Technology, Baghdad 10001, Iraq.

[b] Department of Medical Biochemical Analysis, College of Health Technology, Cihan University-Erbil, Erbil, Kurdistan Region, Iraq

[c] Key Laboratory of Plant Resources Conservation and Sustainable Utilization and Guangdong Provincial Key Laboratory of Applied Botany, South China Botanical Garden, Chinese Academy of Sciences, Guangzhou 510650, People's Republic of China.

[d] Guangzhou HC Pharmaceutical Co., Ltd, Guangzhou 510663, People's Republic of China

[e] Chemistry Science Department, Al-Iraqia University, Baghdad, Iraq.

[f] Department of Pharmaceutical Chemistry, Faculty of Pharmacy, Universitas Airlangga, Jalan Airlangga No. 4-6, Surabaya 60115, Jawa Timur,I ndonesia.

[g] Department of Pharmacy, Faculty of Health Sciences, Muhammadiyah University of Palangkaraya, Palangka Raya 73111, Indonesia

[h] Doctoral Program of Pharmaceutical Sciences, Department of Pharmaceutical Chemistry, Faculty of Pharmacy, Airlangga University, Surabaya 60115, Indonesia

[i] Department of Chemistry, Government College of Engineering, Keonjhar-758002, Odisha, India

**Abstract**

In the present work, we have reported the theoretical and biological activities of some imidazole (MIPBD, CMIBP, MIBPBD) derivatives. Here, the synthesis of one novel substituted imidazo-amino pyridinyl derivative (MIPBD) has also been reported. The structure of this compound was identified by NMR and mass spectroscopy. Molecular modeling studies have confirmed that CMIBP (ΔE= 0.16508 eV) is more stable than others. Antibacterial investigation exhibited good to excellent activity for all these compounds against two tested bacterial strains (*S. aureus* and *E. coli*). Moreover, molecular docking studies were carried out, which was consistent with experimental studies. The results motivate us for further studies of imidazole derivatives which will be helpful for the development of novel antibacterial agents.

*Keywords*: Imidazole; DFT; Antibacterial Activity; Docking; Synthesis

*Corresponding author e-mail: 100416@uotechnology.edu.iq ; (Dhafer S. Zinad); ahmed.mahal@cihanuniversity.edu.iq (Ahmed Mahal)

Received: 26 May 2020; Revised: 30 June 2020; Accepted: 25 August 2020
DOI: 10.21608/EJCHEM.2020.31043.2662

## 1. Introduction

Heterocycles play an important role in drug discovery and medicinal chemistry [1] including the nitrogen-containing heterocycles [2]. Imidazole containing natural products are gaining much interest due to their potent bioactivity and hence, promising agents in drug discovery [3,4] involving anti-bacterial, anti-fungal, anti-cancer, anti-oxidant and anti-parkinson activities [5-7]. For example, Pretomanid and Delamanid were confirmed for their potent anti-TB activity [8-10]. Delamanid has already approved to cure MDR-TB infection while Pretomanid is on the phase III clinical trials [11,12]. Furthermore, novel imidazole derivatives exhibited potent activity at concentrations range (0.5-1.0 mg/mL) against microbial strains in comparison to the positive standard [13].

On the other hand, imidazole scaffolds play an important role in the building block of some biomolecules such as amino acid histidine, biotin, and natural products as well. For instance, Eudistidine C. is a racemic natural product extracted from *Eudistoma sp*. as inhibitor of interaction between the protein binding domains of HIF-1α and p300. In addition, classical procedure to synthesize imidazole ring was described by Heinrich Debus [14]. Recent strategies were often used such as microwave-mediated synthesis [15], *p*-Tosylmethylisocyanide (TosMIC) based imidazole synthesis [16]. The reaction of allenyl sulfonamides with amines resulted 4- and 5-functionalized imidazoles were constructed region selectively depending on the substituents on the nitrogen atoms. [17].

For the importance of using imidazole derivatives in medicinal chemistry as antibacterial agents and herein, we report our effort on the development of one novel aminopyridinyl imidazole derivative and other known two derivatives using 2-chloro-4-cyano pyridine moiety. Furthermore, antibacterial screening and molecular docking studies were investigated to understand these compounds in order to improve their activity as potent antiracial agents. DFT calculations of the synthesized compounds were also doing including the study of stability and reactivity of the synthesized compounds.

## 2. Experimental

### 2.1. Materials

Analytical grade chemicals were used for the present study without further purification. The NMR data were obtained from Bruker ARX NMR spectrometer and Bruker AVANCE III HD NMR spectrometer (BrukerBioSpin AG, Faellanden, Switzerland) at 250 MHz and 300 MHz at ambient temperatures. Chemical shifts were recorded in parts per million (ppm) relative to TMS. Mass spectrum was reported on ESIMS spectrometer (Shimadzu Corporation, Kyoto, Japan) with TLC interface. In addition, to use natural and UV light for visualization (254, 366 nm), fluorescent silica gel 60 F254 plates were used to achieve TLC (Merck, Darmstadt, Germany). HPLC was tested the purity of the targets as more than 95%.

### 2.2. Synthesis of $N^1$-(4-(1-Methyl-1H-imidazol-2-yl)pyridin-2-yl)benzene-1,4-diamine (MIPBD).

The whole compounds 3, CMIBP, MIBPBD have been prepared as described previously [18-29]. A mixture of compound (3) (0.20 g, 1.032 mmol), 4-phenylenediamin (0.167 g, 1.54 mmol) and solution of HCl /ethanol 1.25M (842µL, 1.032 mmol) in n-butanol (5 mL) were heated with stirring in a pressure vial for 16 h at 180°C. The solvent was evaporated at reduced pressure and the residue was purified by flash column chromatography ($SiO_2$, $CH_2Cl_2$/EtOH 95:05) yielded the title compound as yellow oil (0.125 g, 46%). $^1$H NMR (300.13 MHz, DMSO-$d_6$) δ = 3.79 (s, 3H), 4.78 (br. s, 2H), 6.56 (d, J = 8.71 Hz, 2H), 6.93-7.01 (m, 3H), 7.22-7.29 (m, 3H), 8.10 (d, J = 5.32 Hz, 1H), 8.55 ppm (s, 1H). $^{13}$C-NMR (75.47 MHz, DMSO-$d_6$) δ = 35.1, 107.5, 111.8, 114.8, 122.3, 125.0, 128.4, 130.9, 138.9, 144.2, 145.0, 148.3, 157.9 ppm. MS-ESIm/z: $[M+H]^+$ calcd. for $C_{15}H_{15}N_5$: 265.2, found: 266.1; HPLC retention time ($t_R$): = 1.172 minute (100%). Analysis Calculated for $C_{15}H_{15}N_5$: C, 67.90; H, 5.70;

N, 26.40. Found: C, 68.21; H, 5.96; N, 26.66 (Figure 1 and 2).

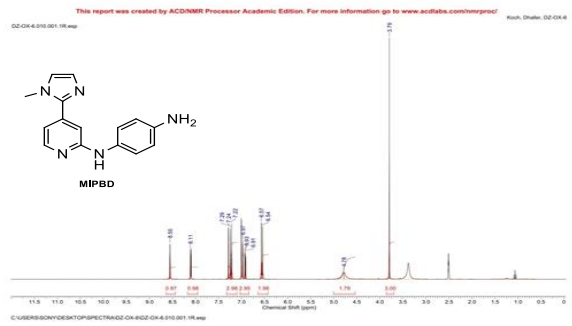


**Figure 1.** $H^1$-NMR spectrum for MIPBD

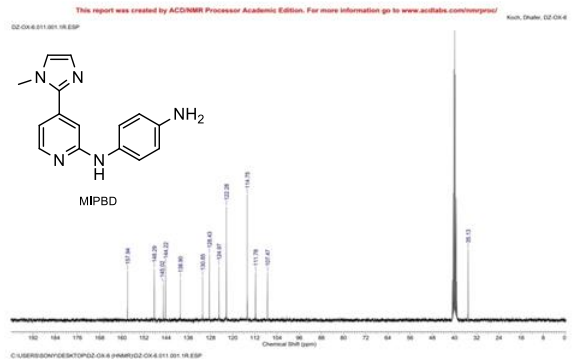


**Figure 2**. $C^{13}$-NMR spectrum for MIPBD

2.3. Antibacterial Activity in vitro

Two bacterial strains including *S. aureus* (G+ve) and *E. coli* (G-ve) were obtained from Applied Science Department at University of Technology, Iraq. The selection of both strains was based on their activity in the treatment of wound infection. Fresh inoculants were prepared on nutrient broth for 24 h at 37 °C. Disk diffusion method on an agar plate was utilized to investigate the antibacterial activity [30,31]. A cultured agar (10 mL) containing mixed samples (1 cm) was inoculated onto 10 µl of microbe culture add incubated for a period of 24 h at 37 °C. Subsequently 25µl, 50 µl, and 100 µl of the synthesized compounds suspensions were loaded into the wells separately. Tetracycline (10 mg) was used as positive control. Dimethylsulfoxide (DMSO) was used as control and no visible inhibition zone was observed on control groups. After the incubation period, the plates were observed for zones of inhibition (in mm).

2.4. Docking Study

The softwares HyperChem 7.5, OpenBabel 2.4.1, AutoDock Tools 1.5.6, AutodockVina 1.1.2, PyMOL 2.3.1, UCSF Chimera 1.13.1, and Discovery Studio Visualizer 19.1.0.18287 were used for the present study [32-35]. The receptor protein is obtained from the protein data bank (https://www.rcsb.org/). HyperChem 7.5 was used to sketch the two-dimensional structure of the tested ligands with geometry optimization *ab initio* basis set 6-31G*. Docking is done by using Autodock Vina 1.1.2 and Discovery Studio Visualizer 19.1.0 is used for two-dimensional observation of the docking results. [36]. The receptor used is the 30S ribosome, the smaller subunit of 70S ribosome found in prokaryotes which is known to be a target for tetracycline interactions, especially in the 16S ribosomal RNA section [37,38]. There are two 30S ribosomal receptor crystals used, each with PDB ID 1HNW [39] and 1I97 [40], both of which have tetracycline as co-crystal ligands with different binding sites. The center coordinates of the grid box are adjusted automatically with the ligand co-crystal position of each receptor [41]. The docking methods and parameters have been validated by re-docking using reference ligands [42]. Lower RMSD value indicates the docking ligand position which is getting closer to the crystallographic results [43]. The main parameters used in docking process were the free binding energy (ΔG) and amino acid residues similarity [41,44]. With discovery studio visualizer v.19.1.0.18287, the docking for all tested ligands [45] is carried out in same way as validation process and ligand-receptor interactions are visualized.

## 3. Results and Discussion

3.1. Chemistry

The synthesis of novel imidazo-aminopyridinyl derivatives starting from 2-chloroisonicotinonitrile (1) are outlined in scheme 1. $N^1$-(4-(1-methyl-1*H*-imidazol-2-yl)pyridin-2-yl)benzene-1,4-diamine (MIPBD) was synthesized starting from compound **3**. The condensation reaction of compound **3** with 4-phenylenediamin using HCl/EtOH as a catalyst in n-butanol as the solvent resulted a yield of 46%. The reaction mixture was stirred and heated for 16 h in a pressure vial at 150°C.

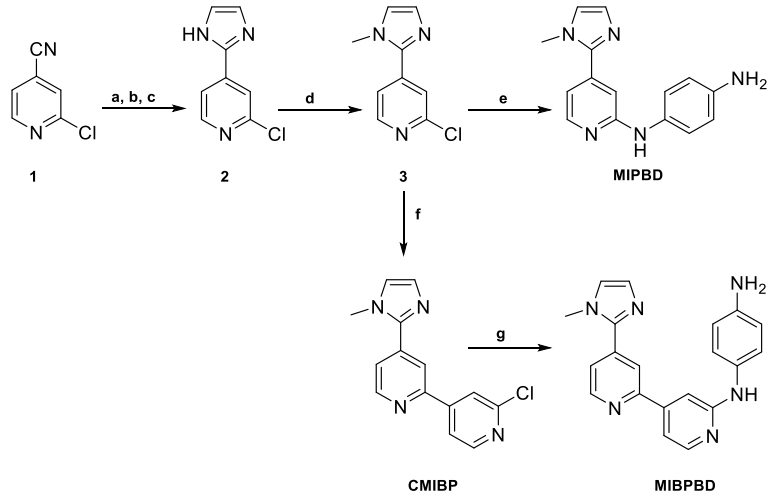


**Reaction reagent and conditions**: (a) 30% Sodium methoxide ($NaOCH_3$) in methanol, $CH_3OH$, 40 °C, 1h. (b) 2,2-Dimethoxyethylamine $NH_2CH_2CH(OCH_3)_2$, acetic acid, $CH_3OH$, reflux, 30 minutes (c) 6M HCl, reflux, 18 h. (d) Methyl iodide ($CH_3I$), Sodium hydride (NaH), dry DMF, room temperature, 2h. (e) 4-phenylenediamin, 1.25M HCl/ethanol, n-butanol, 180°C, 16h. (f) Pd(PPh3)4, (2-chloropyridin-4-yl)boronic acid, $Cs_2CO_3$, dioxane,150 °C, 6h. (g) 4-phenylenediamin,1.25M HCl/ethanol, n-butanol, 180 °C, 16h.

**Scheme 1.** Synthesis of some novelimidazo-aminopyridinyl derivatives

Green route approach using water (80-100ºC) as a solvent has not led to the formation of diphenylamine (entry 4-6) [46]. The slow reaction of 2-chlorpyridine with amines for diphenylamine formation (table 1) required a relatively high temperature and long reaction time.

The $^1$H-NMR spectrum exhibited a broad singlet with chemical shift at δ = 3.79 ppm due to the three protons of methyl amine and two singlet's at δ = 4.78 ppm and 8.11 ppm due to $NH_2$ and NH protons, respectively. Moreover, $^{13}$C NMR spectrum exhibited signals at δ = 35.1 due to methyl amine and 157.9 ppm due to azomethane (–N=C-C=) group. MS-ESI: *m/z* $[M+H]^+$ was found to be 266.1 and the HPLC purity was found (100%) with retention time ($t_R$) appeared at 1.172 min.

3.2. 3D-Molecular Modeling Studies

The molecular modeling studies are essential to understand the molecular arrangement of the compounds. The four compounds 3, CMIBP, MIBPBD and MIPBD were optimized with the help of Becke's three parameters and Lee-Yang-Parr functional (B3LYP)[47] level with 6-311G (d) basis set (figure 3-6).

The calculations and observations were performed by using Gaussian 09 program platform and analyzed with Gauss View 5.0.9 program. Various bond lengths and bond angels have been observed for the whole compounds. The importance of theoretical approach is to explain the chemical reactivity and selection of chemically active site of the compounds during reaction.

**Table 1.** Optimization of MIPBD synthesis reaction c conditions

| Entry | Catalyst | Solvent | Temperature/°C | Time/h | Conversion rate |
|---|---|---|---|---|---|
| 1 | HCL/EtOH | n-butanol | 150 | 16 | 46%[b] |
| 2 | HCL/EtOH | *i*- propanol | 150 | 16 | 25%[a] |
| 3 | HCL/EtOH | MeOH | 150 | 16 | 20%[a] |
| 4 | | $H_2O$ | 80 | 24 | no reaction |
| 5 | | $H_2O$ | 90 | 24 | no reaction |
| 6 | | $H_2O$ | 100 | 24 | no reaction |

[a] conversion rate using TLC estimation; [b] isolated yield after column chromatography purification

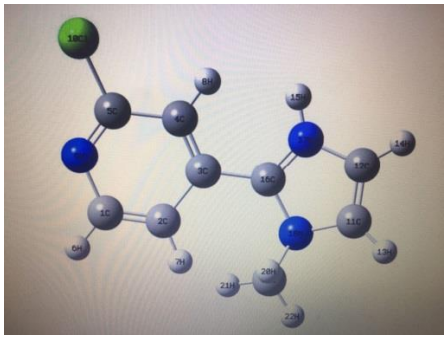

**Figure 3.** Optimized geometry of 3

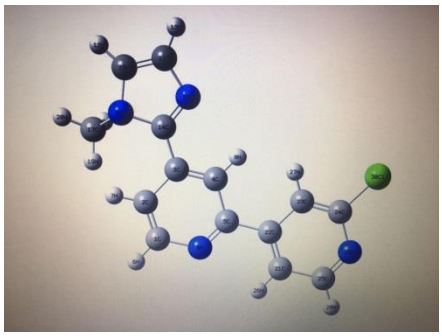

**Figure 5.** Optimized geometry of CMIBP

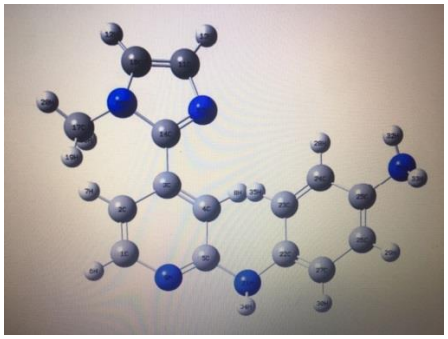

**Figure 4.** Optimized geometry of MIPBD

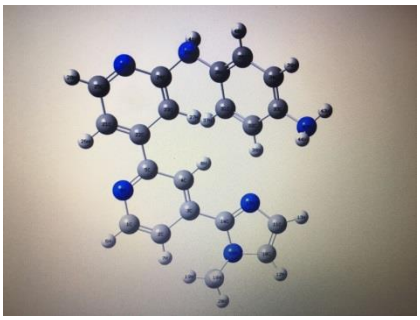

**Figure 6.** Optimized geometry of MIBPBD

According to Frontier Molecular Orbitals approach the energy gap between HOMO and LUMO orbitals explain the electron transfer interaction [48]. Some parameters are called chemical reactivity values such as global hardness (η), chemical potential (μ), electronegativity (χ), global electrophilicity index (ω) and global softness (S) [49].

$$\boldsymbol{\chi = -\frac{(E_{LUMO} + E_{HOMO})}{2}}$$

$$\boldsymbol{\mu = -\chi = \frac{(E_{LUMO} + E_{HOMO})}{2}}$$

$$\boldsymbol{\eta = \frac{(E_{LUMO} - E_{HOMO})}{2}}$$

$$\boldsymbol{S = \frac{1}{2\eta}}$$

$$\boldsymbol{\omega = \frac{\mu^2}{2\eta}}$$

$$\boldsymbol{\sigma = \frac{1}{\eta}}$$

Based on the results listed in table 2, MIBPBD with the highest HOMO energy ($E_{HOMO}$ = -0.18165 eV), lowest potential ionization value (*I* = 0.18165 eV) acts as the best electron donor, while the compound CMIBP with the lowest LUMO energy ($E_{LUMO}$= -0.08054 eV), the highest electron affinity (A= 0.08054 eV), and the highest potential ionization value (*I* = 0.24562 eV) among all of the investigated products acts as the best electron acceptor. Chemical hardness (softness) indicates that MIBPBD (η= 0.060565 eV, S= 8.25559 eV) is the least (greatest) among all of the studied products.

CMIBP (ω= 0.161103eV) has the strongest electrophilic properties among other compounds, according to the results on the electrophilicity index (ω). The smallest frontier orbital gap (ΔE= 0.12113 eV) of MIBPBD (figure 7) among investigated products results from the highest chemical reactivity, most polarizable and least kinetically stable "soft molecule" form.

The reactivity of MIBPBD is greater based on energy gap (ΔE) parameters, which confirmed that CMIBP is the most stable compound compared to others and follow the order: CMIBP>MIPBD>MIBPBD (Figure 7). Furthermore, Global Hardness (η), global softness (S) and the chemical potential (μ) are also important parameters to measure the stability of the compounds.

**Table 2.** Calculated quantum chemical parameters for all compounds

| Parameters | CMIBP | MIPBD | MIBPBD |
|---|---|---|---|
| $E_{HOMO}$ | -0.24562 | -0.18204 | -0.18165 |
| $E_{LUMO}$ | -0.08054 | -0.03821 | -0.06052 |
| $\Delta E_{gap}$ | 0.16508 | 0.14383 | 0.12113 |
| IE | 0.24562 | 0.18204 | 0.18165 |
| A | 0.08054 | 0.03821 | 0.06052 |
| η | 0.08254 | 0.071915 | 0.060565 |
| ω | 0.161103 | 0.084318 | 0.121039 |
| χ | 0.16308 | 0.110125 | 0.121085 |
| μ | -0.16308 | -0.110125 | -0.121085 |
| S | 6.05766 | 6.95265 | 8.25559 |
| σ | 12.115338 | 13.905304 | 16.511186 |
| | **Single point energy of ligand** | | |
| | Energy (A.U) | Dipole moment (D) | |
| CMIBP | 1180.410909 | 9.6067 | |
| MIPBD | -810.99678 | 6.7189 | |
| MIBPBD | -1061.727104 | 10.0175 | |

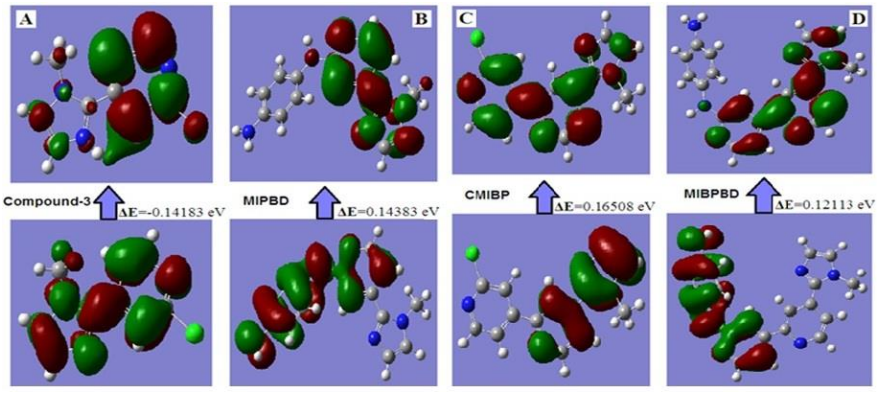


**Figure 7.** HOMO-LUMO energy gap of (A) Compound 3, (B) MIPBD, (C) CMIBP and (D) MIBPBD

3.3. Antibacterial Activity

The imidazole derivatives were evaluated for their antibacterial activities against the bacterial strains *S. aureus* and *E coli*. Tetracycline is used as the positive reference. The targets showed considerable activity against the bacterial strains (Figure 8). The compound MIBPBD and MIPBD showed excellent activity against both the strains while, CMIBP showed less activity. A synergistic effect involving the aniline moiety and secondary amine might be responsible for this enhancement. The mode of action of the compounds may include the formation of a hydrogen bond with the active centers of cell constituents through the amino group ($NH_2$), interfering with the normal cell and causing death of bacteria [31].

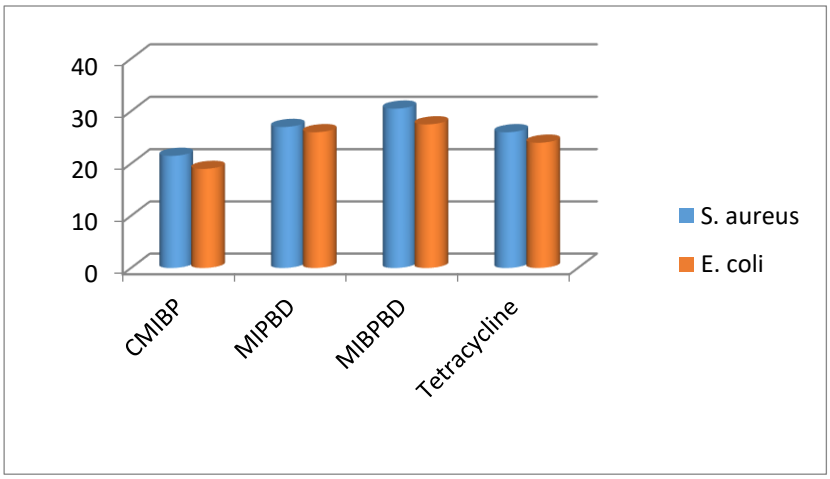


**Figure 8**. Antibacterial activity of these imidazole derivatives (ZI in mm)

3.4. Docking validation protocol

RMSD scores of 13.633 Å for 1HNW and 14.304 Å for 1I97 were provided for the re-docking results from this study. This value tends to be high because generally for molecular docking, the RMSD value specified for the validation process is usually not more than 2 Å [50]. However, this value is obtained by using the least-sized grid box that can still contain both co-crystal and tested ligands. The RMSD value can be increased by reducing the size of the grid box used. However, this will result in the grid box size being too small and unable to load the ligand used [51]. One of the factors causing the RMSD scores to be high is the presence of solvent molecules such as magnesium ions at the binding site of both receptors. During the crystallographic process, the solvent molecule also interacts with the co-crystal ligand so that it affects the position of the co-crystal ligand. While in the docking process, the solvent molecule is removed, hence a shift in the position of the ligand by filling in the position left by the previous solvent molecule [52]. The docking process is therefore performed using the dimensions and size of the grid box used for the process validation. In addition to the grid box coordinates and size, amino acid residues and ΔG were identified (table 3).

**Table 3.** Validation Process Results

| Parameters | Value | |
|---|---|---|
| PDB ID | 1HNW | 1I97 |
| Reference ligand | Tetracycline | Tetracycline |
| Grid box size (Å) | 30 x 30 x 30 | 30 x 30 x 30 |
| Grid box position | x: 205.502 | x: 24.919 |
| | y: 109.132 | y: 96.765 |
| | z: 4.235 | z: 156.574 |
| RMSD (Å) | 13.633 | 14.304 |
| ΔG (kcal/mol) | -9.1 | -9.3 |
| Amino acid residues | - | 2-Gly[b] |
| | 163-Ala[a] | - |
| | 164-Arg[b] | - |
| | - | 1035-G[b] |
| | - | 1036-C[b] |
| | - | 1039-G[b] |
| | - | 1041-C[b] |
| | - | 1042-C[b] |
| | - | 1043-G[a] |
| | - | 1044-U[a] |
| | 1053-G[a] | - |
| | 1054-C[b] | - |
| | 1056-U[a] | - |
| | 1057-G[b] | - |
| | 1058-G[b] | - |
| | 1059-C[b] | - |
| | 1060-C[b] | - |
| | - | 1174-G[a] |
| | - | 1175-U[a] |
| | - | 1176-C[b] |
| | - | 1177-U[a] |
| | - | 1178-G[a] |
| | - | 1179-G[a] |
| | - | 1180-U[b] |
| | 1194-U[b] | - |
| | 1195-C[b] | - |
| | 1196-U[a] | - |
| | 1197-G[a] | - |
| | 1198-G[b] | - |
| | 1199-U[b] | - |

[a]Hydrogen bond; [b]Van der Waals interaction

## 3.5. Molecular Docking Study

All the tested ligands have been docked and formed a consistent pattern: ranking of ΔG values shown for 1HNW and 1I97 are of exact same order, as presented in Table 4 and 5. In addition, the rank of the test ligand is almost similar to that obtained from the antibacterial test results *in vitro*, where the highest potential is shown by compound MIBPBD. In fact, like the results of *in vitro* tests where compound MIBPBD has a slightly larger zone of bacterial inhibition than tetracycline (3.5-4.5 mm), compound MIBPBD also has a slightly lower ΔG value (0.5 kcal/mol) compared to tetracycline as a reference ligand. These results reinforce while explaining the *in vitro* results that have been obtained previously, where the difference in interactions shown at each binding site of the 30S ribosome is one of the factors that influence the antibacterial activity of the test compounds [53]. The interesting point is that at 1HNW receptor, compound MIBPBD is one of the ligands that has the fewest interactions (of five nitrogen bases with six interactions). While at receptor 1I97, compound MIBPBD actually shows the most interactions (of six nitrogen bases with eight interactions). In fact, when viewed in terms of molecular size, compound MIBPBD has a larger size than other ligands, so it is natural to have a higher

number of interactions [54]. But still in both binding sites compound MIBPBD shows the lowest ΔG value with a difference of 1.3 - 1.7 kcal/mol with other ligands. In other words, a greater number of interactions cannot always be associated with lower ΔG values. There are other factors that also play a role in the interaction between the ligand and the binding site of the receptor, such as the interaction between the ligand pharmacophore group and certain key amino acids/nitrogen bases of the receptor [55]. In this case, especially at the 1HNW receptor, compound MIBPBD interacts with several key nitrogen bases that do not occur in other test ligands such as 966-G, 1054-C, 1196-U, and 1198-G. Of the four nitrogen bases, three of them also occur in tetracycline from the previous re-docking result. In other words, the four nitrogen bases play an important role in the interaction of antibacterial compounds on the 30S ribosome at the binding site.

**Table 4.** Results of test ligands docked at 1HNW receptor binding site

| Parameters | MIPBD | | CMIBP | | MIBPBD | |
|---|---|---|---|---|---|---|
| | Value | Distance (Å) | Value | Distance (Å) | Value | Distance (Å) |
| ΔG (kcal/mol) | -8.3 | - | -8.0 | - | -9.6 | - |
| Amino acid residues | - | - | 162-Gln[b] | 2.55 | - | - |
| | - | - | 163-Ala[b] | 2.12 | - | - |
| | - | - | - | - | - | - |
| | - | - | - | - | 966-G[b] | 2.04 |
| | 1053-G[a] | 3.54 | 1053-G[b] | 1.82 | 1053-G[a] | 3.62 |
| | 1053-G[a] | 3.75 | 1053-G[b] | 2.69 | 1053-G[d] | 4.30 |
| | - | - | 1053-G[a] | 3.62 | - | - |
| | - | - | - | - | 1054-C[b] | 2.46 |
| | 1056-G[a] | 3.32 | - | - | - | - |
| | 1057-G[d] | 4.47 | 1057-G[b] | 2.31 | - | - |
| | - | - | - | - | - | - |
| | - | - | 1194-U[a] | 3.58 | - | - |
| | - | - | 1194-U[a] | 3.73 | - | - |
| | 1195-C[d] | 3.35 | 1195-C[a] | 3.57 | - | - |
| | - | - | - | - | 1196-U[b] | 2.57 |
| | - | - | 1197-G[a] | 3.73 | - | - |
| | - | - | - | - | 1198-G[b] | 2.10 |
| | 1199-U[b] | 2.24 | 1199-U[b] | 2.99 | - | - |

[a]Carbon Hydrogen bond; [b]Conventional Hydrogen bond; [c]Pi-alkyl Interaction; [d]Pi-cation/anion Interaction.

While at the binding site of the 1I97 receptor, there are two nitrogen bases which do not interact with other test ligands, which are 1176-C and 1379-C. Of the two, only one interacted with tetracycline, 1176-C. In other words, the unique interaction on 1379-C might have contributed to the low ΔG value of compound MIBPBD against the 30S ribosome at the binding site. The visualization of the docking results for each test ligand on the two receptors is shown in figure 9 for clearer observation.

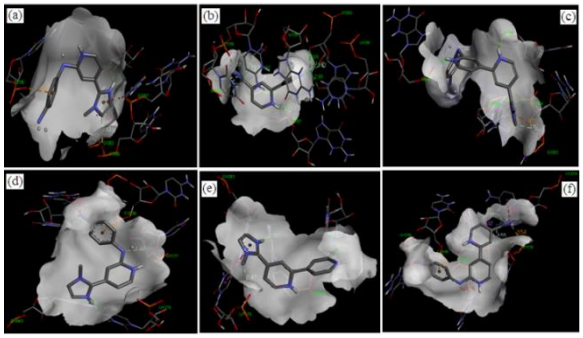


**Figure 9.** Docked conformation of (a) MIPBD, (b) CMIBP, (c) MIBPBD at the 30S ribosome receptor with PDB ID 1HNW and Docked conformation of (d) MIPBD, (e) CMIBP, (f) MIBPBD at the 30S ribosome receptor with PDB ID 1I97.

**Table 5.** Docking results of test ligands at 1I97 receptor binding site

| Parameters | MIPBD | | CMIBP | | MIBPBD | |
|---|---|---|---|---|---|---|
| | Value | Distance (Å) | Value | Distance (Å) | Value | Distance (Å) |
| ΔG (kcal/mol) | -8.1 | - | -8.0 | - | -9.8 | - |
| Amino acid residues | - | - | - | - | - | - |
| | - | - | - | - | - | - |
| | - | - | - | - | - | - |
| | - | - | - | - | - | - |
| | 1035-G[d] | 2.98 | - | - | 1035-G[d] | 2.93 |
| | 1035-G[d] | 3.25 | - | - | - | - |
| | 1036-C[e] | 3.37 | - | - | 1036-C[e] | 3.98 |
| | 1043-G[b] | 2.69 | 1043-G[b] | 2.05 | - | - |
| | - | - | 1043-G[b] | 2.81 | - | - |
| | 1175-U[b] | 2.02 | 1175-U[a] | 3.47 | - | - |
| | - | - | 1175-U[c] | 5.41 | - | - |
| | - | - | - | - | 1176-C[e] | 3.54 |
| | - | - | - | - | 1176-C[a] | 3.55 |
| | 1177-U[a] | 3.48 | - | - | 1177-U[g] | 3.87 |
| | - | - | 1178-G[b] | 2.05 | 1178-G[d] | 1.35 |
| | 1180-U[b] | 3.01 | 1180-U[f] | 3.14 | - | - |
| | - | - | - | - | 1379-C[a] | 3.54 |
| | - | - | - | - | 1379-C[c] | 5.37 |

[a]Carbon Hydrogen bond; [b]Conventional Hydrogen bond; [c]Pi-Pi T-shaped Interaction; [d]Unfavourable Donor-Donor Interaction; [e]Pi-anion Interaction; [f]Halogen bond; [g]Pi-sigma Interaction.

## 4. Conclusion

A variety of imidazole derivatives involving CMIBP, MIBPBD and MIPBD have been synthesized using an easy and versatile synthetic strategy from 2-chloroisonicotinonitrile as starting material. The structural elucidations of the compounds were carried out by using several physico-analytical techniques. The purity of these compounds was checked by HPLC method. In addition, theoretical calculation including DFT study revealed that the reactivity of MIBPBD is highest based on energy gap (ΔE) parameters and it was also concluded that CMIBP is the most stable compared to others as shown in the order CMIBP>MIPBD>MIBPBD. The antibacterial activity of all these derivatives showed potent activity against *S. aureus* and *E. coli* compared to positive reference tetracycline antibiotic. The docking results showed similarity in rank to those shown in the *in vitro* test, where MIBPBD has lowest ΔG value.

## 5. Conflicts of interest

There is no conflict of interest.

## 6. Acknowledgement

This study was supported by the University of Technology, Baghdad, Iraq. Ahmed Mahal acknowledges the Chinese Academy of Sciences (CAS) for financial support through the CAS President's International Fellowship Initiative (2016PM032) and Cihan University as well.

## 7. References

[1] a) Zinad, D. S., Mahal, A., Mohapatra, R. K., Sarangi, A. K., Pratama, M. R.F., Medicinal chemistry of oxazines as promising agents in drug discovery. *Chemical Biology & Drug Design*, **95**(1), 16-47 (2020). doi.org/10.1111/cbdd.13633

b) Mahal, A., Oxetanes as versatile building blocks in the total synthesis of natural products: An overview. *European Journal of Chemistry*, **6**(3), 357-366 (2015). doi.org/10.5155/eurjchem.6.3.357-366.1267

[2] Mahal, A., Wu, P., Jiang, Z. H., & Wei, X., Synthesis and cytotoxic activity of novel tetrahydrocurcumin derivatives bearing pyrazole moiety. *Natural products and bioprospecting*, **7**(6), 461-469 (2017). doi.org/10.1007/s13659-017-0143-9

[3] Zhang, L., Peng, X. M., Damu, G. L., Geng, R. X., & Zhou, C. H., Comprehensive review in current developments of imidazole-based medicinal chemistry. *Medicinal research reviews*, **34**(2), 340-437 (2014). doi.org/10.1002/med.21290

[4] Jin, Z., Muscarine, imidazole, oxazole, and thiazole alkaloids. *Natural Product Reports*, **28**(6), 1143-1191 (2011). doi.org/10.1039/c0np00074d

[5] Emami, S., Foroumadi, A., Falahati, M., Lotfali, E., Rajabalian, S., Ebrahimi, S., Farahyar, S., Shafiee, A., 2-Hydroxyphenacyl azoles and related azolium derivatives as antifungal agents. *Bioorganic & medicinal chemistry letters*, **18**(1), 141-146 (2008). doi.org/10.1016/j.bmcl.2007.10.111

[6] Pandey, J., Tiwari, V. K., Verma, S. S., Chaturvedi, V., Bhatnagar, S., Sinha, S., Gaikwad, A.N., Tripathi, R. P.. Synthesis and antitubercular screening of imidazole derivatives. *European journal of medicinal chemistry*, **44**(8), 3350-3355 (2009). doi.org/10.1016/j.ejmech.2009.02.013

[7] Nieri, P., Carpi, S., Fogli, S., Polini, B., Breschi, M. C., & Podestà, A., Cholinesterase-like organocatalysis by imidazole and imidazole-bearing molecules. *Scientific reports*, **7**, 45760 (2017). doi.org/10.1038/srep45760

[8] Xu, Z., Gao, C., Ren, Q. C., Song, X. F., Feng, L. S., & Lv, Z. S., Recent advances of pyrazole-containing derivatives as anti-tubercular agents. *European Journal of Medicinal Chemistry***, 139**, 429-440 (2017). doi.org/10.1016/j.ejmech.2017.07.059

[9] Lewis, J. M., & Sloan, D. J., The role of delamanid in the treatment of drug-resistant tuberculosis. *Therapeutics and clinical risk management*, **11**, 779 (2015). doi.org/10.2147/TCRM.S71076

[10] Fan, Y. L., Wu, J. B., Cheng, X. W., Zhang, F. Z., & Feng, L. S., Fluoroquinolone derivatives and their anti-tubercular activities. *European journal of medicinal chemistry*, **146**, 554-563 (2018). doi.org/10.1016/j.ejmech.2018.01.080

[11] Chetty, S., Ramesh, M., Singh-Pillay, A., & Soliman, M. E., Recent advancements in the development of anti-tuberculosis drugs. *Bioorganic & medicinal chemistry letters*, **27**(3), 370-386 (2017). doi.org/10.1016/j.bmcl.2016.11.084

[12] Fan, Y. L., Jin, X. H., Huang, Z. P., Yu, H. F., Zeng, Z. G., Gao, T., & Feng, L. S., Recent advances of imidazole-containing derivatives as anti-tubercular agents. *European journal of medicinal chemistry*, **150**, 347-365 (2018). doi.org/10.1016/j.ejmech.2018.03.016

[13] Gaba, M., Singh, D., Singh, S., Sharma, V., & Gaba, P., Synthesis and pharmacological evaluation of novel 5-substituted-1-(phenylsulfonyl)-2-methylbenzimidazole derivatives as anti-inflammatory and analgesic agents. European journal of medicinal chemistry, **45**(6), 2245-2249 (2010). doi.org/10.1016/j.ejmech.2011.05.005

[14] Debus, H., & Liebigs, S., Synthesis of 2, 2'-imidazole. *Liebigs Ann Chem*, **107**, 199-208 (1858). doi.org/10.1002/jlac.18581070209

[15] Wolkenberg, S. E., Wisnoski, D. D., Leister, W. H., Wang, Y., Zhao, Z., & Lindsley, C. W., Efficient synthesis of imidazoles from aldehydes and 1, 2-diketones using microwave irradiation. *Organic Letters*, **6**(9), 1453-1456 (2004). doi.org/10.1021/ol049682b

[16] Fodili, M., Nedjar-Kolli, B., Garrigues, B., Lherbet, C., & Hoffmann, P., Synthesis of imidazoles from ketimines using tosylmethyl isocyanide (TosMIC) catalyzed by bismuth triflate. *Letters in Organic Chemistry*, **6**(5), 354-358 (2009). doi.org/10.2174/157017809788681275

[17] Yu, L., Deng, Y., & Cao, J., Regioselective synthesis of highly substituted imidazoles via the sequential reaction of allenyl sulfonamides and amines. *The Journal of Organic Chemistry*, **80**(9), 4729-4735 (2015). doi.org/10.1021/acs.joc.5b00141

[18] Ansideri, F., Macedo, J.T., Eitel, M., El-Gokha, A., Zinad, D.S., Scarpellini, C., Kudolo, M., Schollmeyer, D., Boeckler, F.M., Blaum, B.S. and Laufer, S.A., Structural Optimization of a Pyridinylimidazole scaffold: shifting the selectivity from p38α mitogen-activated protein kinase to c-Jun N-terminal kinase 3. *ACS omega*, **3**(7), 7809-7831 (2018). doi.org/10.1021/acsomega.8b00668

[19] Zinad, D. S., AL-Duhaidahaw, D. L., Al-Amiery, A., & Kadhum, A. A. H., N-[4-(1-Methyl-1H-imidazol-2-yl)-2, 4′-bipyridin-2′-yl] benzene-1, 4-diamine. *Molbank*, **2018**(4), M1030 (2018). doi.org/10.3390/M1030

[20] Zinad, D. S., AL-Duhaidahaw, D. L., & Al-Amiery, A., 2′-Chloro-4-(1-methyl-1H-imidazol-2-yl)-2, 4′-bipyridine. *Molbank*, **2019**(1), M1040 (2019). doi.org/10.3390/M1040

[21] Zinad, D. S., Feist, H., Villinger, A., & Langer, P., Suzuki–Miyaura reactions of the bis (triflates) of 1, 3- and 1, 4-dihydroxythioxanthone. Electronic and steric effects on the site-selectivity. *Tetrahedron*, **68(**2), 711-721 (2012). doi.org/10.1016/j.tet.2011.10.095

[22] Zinad, D. S., Hussain, M., Villinger, A., & Langer, P., Site-Selective Synthesis of Arylated Indenones by Suzuki–Miyaura Cross-Coupling Reactions of 2, 3, 5-Tribromoinden-1-one. European Journal of Organic Chemistry, **2011**(22), 4212-4221 (2011). doi.org/10.1002/ejoc.201100313

[23] Ibad, M. F., Hussain, M., Ali, A., Ullah, I., Zinad, D. S., & Langer, P., One-Pot Synthesis of Unsymmetrical 2, 3-Diarylindoles by Site-Selective Suzuki-Miyaura Reactions of N-Methyl-2, 3-dibromoindole. *Synlett*, **2010**(03), 411-414. (2010). doi.org/10.1055/s-0029-1219201

[24] Ibad, M. F., Zinad, D. S., Hussain, M., Ali, A., Villinger, A., & Langer, P., One-pot synthesis of arylated 1-methyl-1H-indoles by Suzuki–Miyaura cross-coupling reactions of 2, 3-dibromo-1-methyl-1H-indole and 2, 3, 6-tribromo-1-methyl-1H-indole. *Tetrahedron*, **69**(35), 7492-7504 (2013). doi.org/10.1016/j.tet.2013.05.100

[25] Mahal, A., Villinger, A., & Langer, P., Synthesis of 1, 2-Diarylanthraquinones by Site-Selective Suzuki-

Miyaura Reactions of the Bis (triflate) of Alizarin. *Synlett*, **2010**(07), 1085-1088 (2010). doi.org/10.1055/s-0029-1219586

[26] Mahal, A., Villinger, A., & Langer, P., Site-Selective Arylation of Alizarin and Purpurin Based on Suzuki–Miyaura Cross-Coupling Reactions. *European Journal of Organic Chemistry*, **2011**(11), 2075-2087 (2011). doi.org/10.1002/ejoc.201001497

[27] Eleya, N., Mahal, A., Hein, M., Villinger, A., & Langer, P., Synthesis of Arylated Quinolines by Chemo-and Site-selective Suzuki–Miyaura Reactions of 5, 7-Dibromo-8-(trifluoromethanesulfonyloxy) quinoline. *Advanced Synthesis & Catalysis*, **353**(14-15), 2761-2774 (2011). doi.org/10.1002/adsc.201100165

[28] Salman, G. A., Mahal, A., Shkoor, M., Hussain, M., Villinger, A., & Langer, P., Regioselective Suzuki–Miyaura reactions of the bis (triflate) of 1, 2, 3, 4-tetrahydro-9, 10-dihydroxyanthracen-1-one. *Tetrahedron Letters*, **52**(3), 392-394 (2011). doi.org/10.1016/j.tetlet.2010.11.052

[29] Ibad, M. F., Eleya, N., Obaid-Ur-Rahman, A., Mahal, A., Hussain, M., Villinger, A., & Langer, P., Site-Selective Suzuki-Miyaura Reactions of 1, 4-and 3, 5-Bis (trifluoromethylsulfonyloxy)-2-naphthoates. *Synthesis*, **2011**(13), 2101-2116 (2011). doi.org/10.1055/s-0030-1260054

[30] Aysha, T., El-Sedik, M., Abd El Megied, S., Ibrahim, H., Youssef, Y., & Hrdina, R., Synthesis, spectral study and application of solid state fluorescent reactive disperse dyes and their antibacterial activity. *Arabian journal of chemistry*, **12**(2), 225-235 (2019). doi.org/10.1016/j.arabjc.2016.08.002

[31] Mahal, A., Abu-El-Halawa, R., Zabin, S. A., Ibrahim, M., Al-Refai, M., & Kaimari, T., Synthesis, characterization and antifungal activity of some metal complexes derived from quinoxaloylhydrazone. *World Journal of Organic Chemistry*, **3**(1), 1-8 (2015). doi.org/10.12691/wjoc-3-1-1

[32] Trott, O., & Olson, A. J., AutoDock Vina: improving the speed and accuracy of docking with a new scoring function, efficient optimization, and multithreading. *Journal of computational chemistry*, **31**(2), 455-461 (2010). doi.org/10.1002/jcc.21334

[33] O'Boyle, N. M., Banck, M., James, C. A., Morley, C., Vandermeersch, T., & Hutchison, G. R., Open babel: an open chemical toolbox. J Cheminf 3(1): 33 (2011). doi.org/10.1186/1758-2946-3-33

[34] Yuan, S., Chan, H. S., & Hu, Z.. Using PyMOL as a platform for computational drug design. *Wiley Interdisciplinary Reviews: Computational Molecular Science*, **7**(2), e1298 (2017). doi.org/10.1002/wcms.1298

[35] Pettersen, E. F., Goddard, T. D., Huang, C. C., Couch, G. S., Greenblatt, D. M., Meng, E. C., & Ferrin, T. E., UCSF Chimera—a visualization system for exploratory research and analysis. *Journal of computational chemistry*, **25**(13), 1605-1612 (2004). doi.org/10.1002/jcc.20084

[36] Forli, S., Charting a path to success in virtual screening. *Molecules*, **20**(10), 18732-18758 (2015). doi.org/10.3390/molecules201018732

[37] Chukwudi, C. U., rRNA binding sites and the molecular mechanism of action of the tetracyclines. *Antimicrobial agents and chemotherapy*, **60**(8), 4433-4441 (2016). doi.org/10.1128/AAC.00594-16

[38] Hong, W., Zeng, J., & Xie, J., Antibiotic drugs targeting bacterial RNAs. *Acta Pharmaceutica Sinica B*, **4**(4), 258-265 (2014). doi.org/10.1016/j.apsb.2014.06.012

[39] Brodersen, D. E., Clemons Jr, W. M., Carter, A. P., Morgan-Warren, R. J., Wimberly, B. T., & Ramakrishnan, V., The structural basis for the action of the antibiotics tetracycline, pactamycin, and hygromycin B on the 30S ribosomal subunit. *Cell*, **103**(7), 1143-1154 (2000). doi.org/10.1016/s0092-8674(00)00216-6

[40] Pioletti, M., Schlünzen, F., Harms, J., Zarivach, R., Glühmann, M., Avila, H., Bashan, A., Bartels, H., Auerbach, T., Jacobi, C. and Hartsch, T., Crystal structures of complexes of the small ribosomal subunit with tetracycline, edeine and IF3. *The EMBO journal*, **20**(8), 1829-1839 (2001). doi.org/10.1093/emboj/20.8.1829

[41] Forli, S., Huey, R., Pique, M. E., Sanner, M. F., Goodsell, D. S., & Olson, A. J., Computational protein–ligand docking and virtual drug screening with the AutoDock suite. *Nature protocols*, **11**(5), 905-919 (2016). doi.org/10.1038/nprot.2016.051

[42] Meng, X. Y., Zhang, H. X., Mezei, M., & Cui, M., Molecular docking: a powerful approach for structure-based drug discovery. Curr Comp Aided Drug Des **7** (2): 146–157 (2011). doi.org/10.2174/157340911795677602

[43] Pagadala, N. S., Syed, K., & Tuszynski, J., Software for molecular docking: a review. *Biophysical reviews*, **9**(2), 91-102 (2017). doi.org/10.1007/s12551-016-0247-1

[44] Natesan, S., Subramaniam, R., Bergeron, C., & Balaz, S., Binding affinity prediction for ligands and receptors forming tautomers and ionization species: inhibition of mitogen-activated protein kinase-activated protein kinase 2 (MK2). *Journal of medicinal chemistry*, **55**(5), 2035-2047 (2012). doi.org/10.1021/jm201217q

[45] Singh, H., Srivastava, H. K., & Raghava, G. P., A web server for analysis, comparison and prediction of protein ligand binding sites. *Biology direct*, **11**(1), 14 (2016). doi.org/10.1186/s13062-016-0118-5

[46] Mahal, A., Wu, P., Jiang, Z. H., & Wei, X., Schiff bases of tetrahydrocurcumin as potential anticancer agents. *ChemistrySelect*, **4**(1), 366-369 (2019). doi.org/10.1002/slct.201803159

[47] Gill, P. M., Johnson, B. G., Pople, J. A., & Frisch, M. J., The performance of the Becke-Lee-Yang-Parr (B-

LYP) density functional theory with various basis sets. *Chemical Physics Letters*, **197**(4-5), 499-505 (1992). doi.org/10.1016/0009-2614(92)85807-m

[48] M. J. Frisch, G. W. Trucks, H. B. Schlegel, G. E. Scuseria, M. A. Robb, J. R. Cheeseman, G. Scalmani, V. Barone, B. Mennucci, G. A. Petersson, H. Nakatsuji, M. Caricato, X. Li, H. P. Hratchian, A. F. Izmaylov, J. Bloino, G. Zheng, J. L. Sonnenberg, M. Hada, M. Ehara, K. Toyota, R. Fukuda, J. Hasegawa, M. Ishida, T. Nakajima, Y. Honda, O. Kitao, H. Nakai, T. Vreven, J. A. Montgomery, Jr., J. E. Peralta, F. Ogliaro, M. Bearpark, J. J. Heyd, E. Brothers, K. N. Kudin, V. N. Staroverov, R. Kobayashi, J. Normand, K. Raghavachari, A. Rendell, J. C. Burant, S. S. Iyengar, J. Tomasi, M. Cossi, N. Rega, J. M. Millam, M. Klene, J. E. Knox, J. B. Cross, V. Bakken, C. Adamo, J. Jaramillo, R. Gomperts, R. E. Stratmann, O. Yazyev, A. J. Austin, R. Cammi, C. Pomelli, J. W. Ochterski, R. L. Martin, K. Morokuma, V. G. Zakrzewski, G. A. Voth, P. Salvador, J. J. Dannenberg, S. Dapprich, A. D. Daniels, O. Farkas, J. B. Foresman, J. V. Ortiz, J. Cioslowski, D. J. Fox, Gaussian 09, Revision A.02, Gaussian, Inc., PA, Wallingford CT., **28**, 200 (2009).

[49] Peters, J. W., Lanzilotta, W. N., Lemon, B. J., & Seefeldt, L. C., X-ray crystal structure of the Fe-only hydrogenase (CpI) from Clostridium pasteurianum to 1.8 angstrom resolution. *Science*, **282**(5395), 1853-1858 (1998). doi.org/10.1126/science.282.5395.1853

[50] Hevener, K. E., Zhao, W., Ball, D. M., Babaoglu, K., Qi, J., White, S. W., & Lee, R. E., Validation of molecular docking programs for virtual screening against dihydropteroate synthase. *Journal of chemical information and modeling*, **49**(2), 444-460 (2009). doi.org/10.1021/ci800293n

[51] Feinstein, W. P., & Brylinski, M. Calculating an optimal box size for ligand docking and virtual screening against experimental and predicted binding pockets. *J Cheminform*. **7**: 18 (2015). doi.org/10.1186/s13321-015-0067-5

[52] Deller, M. C., & Rupp, B., Models of protein–ligand crystal structures: trust, but verify. *Journal of computer-aided molecular design*, **29**(9), 817-836 (2015). doi.org/10.1007/s10822-015-9833-8

[53] Polikanov, Y. S., Aleksashin, N. A., Beckert, B., & Wilson, D. N., The mechanisms of action of ribosome-targeting peptide antibiotics. *Frontiers in molecular biosciences*, **5**, 48 (2018). doi.org/10.3389/fmolb.2018.00048

[54] Malhotra, S., & Karanicolas, J., When does chemical elaboration induce a ligand to change its binding mode?. *Journal of medicinal chemistry*, **60**(1), 128-145 (2017). doi.org/10.1021/acs.jmedchem.6b00725

[55] Mishra, A., & Dey, S., Molecular Docking Studies of a Cyclic Octapeptide-Cyclosaplin from Sandalwood. *Biomolecules*, **9**(11), 740 (2019). doi.org/10.3390/biom9110740